検体を除いた後に超高純度 He ガスを約 50 mL/min の流速で流しながらチャンバーを室温から 200°C まで 1 時間にわたって加熱し、チャンバー内の蓋部分に吸着した SVOC を脱着して Tenax TA 吸着管に捕集した。

Tenax TA 吸着管に捕集した VOC は、加熱脱離-GC/MS (Shimadzu TD-20 及び GCMS-2010Ultra) で定量した。室内空気分析用 50VOCS 標準液 (Supelco 社製) を段階希釈して検量線を作成した。加熱脱離-GC/MS 分析の主要な測定条件を以下に記した。

[Thermal Desorption]
Desorption: 280°C, 10 min, 50 mL He/min
Cold Trap: -15°C
Trap Desorption: 280°C, 10 min
Line and Valve Temp.: 250°C
[GC]
Column: Rtx-1 (0.32 mm x 60 m, 1 μm)
Carrier Gas: He, 40 cm/min
Split Ratio: 1:20
Oven Temp: 40°C - 5°C /min - 250°C (3 min)
[MS]
Interface Temp.: 250°C
Ion Source Temp.: 200°C
Scan range: *m/z* 35-400

Tenax TA 吸着管に捕集した SVOCs は、加熱脱離-GC/MS (Shimadzu TDTS-2010 及び GCMS-2010) を用い、FASST (Fast Automated Scan/SIM Type) モードで測定した。測定対象物質としてフタル酸エステル 4 化合物 (Diethyl Phthalate (DEP), Dibutyl Phthalate (DBP), Benzyl Butyl (BBP) 及び bis(2-Ethylhexyl) Phthalates (DEHP),アジピン酸エステル類 3 化合物 (Disiobutyl Adipate (DiBA), Dibutyl Adipate (DBA) 及び Dioctyl Adipate (DOA)), リン酸トリエステル類 5 化合物 (Triethyl Phosphate (TEP), Tributyl Phosphate (TBP), tris(2-Chloroethyl) Phosphate (TCEP), Triphenyl Phosphate (TPhP) 及び tris(2-Eethylhexyl) Phosphates (TEHP)) を選定し、1 ng から 400 ng の範囲で定量した。加熱脱離-GC/MS 分析の主要な測定条件を以下に記す。

[Thermal Desorption]
Desorption: 300°C, 10 min, 50 mL He/min
Cold Trap: -10°C
Trap Desorption: 300°C, 10 min
Line and Valve Temp.: 300°C
[GC]
Column: Rtx-1 (0.32 mm x 60 m, 1 μm)
Carrier Gas: He, 30cm/min
Split Ratio: 1:20
Oven Temp.: 80°C - 40°C /min - 200°C - 5°C /min - 320°C (5 min)
[MS]
Interface Temp.: 250°C
Ion Source Temp.: 230°C
Scan range: *m/z* 50-500
Monitor Ions: TEP (99, 155), DEP (149, 177), TBP (99, 155), DiBA (129, 185), TCEP (249, 251), DBA (129, 185), DBP (149, 223), BBP (149, 206), DOA (129, 147), TPhP (326, 325), TEHP (99, 113), DEHP (149, 279)

B-3 4 連チャンバー型 μ-CTE 放散試験による形態別 SVOC 放散量の評価法 (平成 24 年度)

フタル酸エステル類 5 化合物 (Dibutyl Phthalate, Benzyl Butyl Phthalate, Bis(2-ethylhexyl) Phthalate, Di-n-octyl Phthalate, Dinonyl Phthalate)、リン酸トリエステル類 14 化合物 (Triethyl Phosphate, Tripropyl Phosphate, Tributyl Phosphate, Tris(2-chloroethyl) Phosphate, Tris(1,3-dichloroisopropyl) Phosphate, Tri(butoxyethyl) Phosphate, Triphenyl Phosphate, Isodecyl Diphenyl Phosphate, Di-n-octyl Phenyl Phosphate, Tris(2-ethylhexyl) Phosphate, Tris(2-chloroisopropyl) Phosphate, Cresyl Diphenyl Phosphate, Bis(4-methylphenyl) Phenyl Phosphate, Tricresyl Phosphate)、アジピン酸エステル類 3 化合物 (Dibutyl Adipate, Bis(2-ethylhexyl) Adipate, Dinonyl Adipate)、及びその他の可塑剤として 3 化合物 (TXIB, Bis(2-ethylhexyl) Terephthalate, Hexamoll DINCH) の計 25 化合

物を測定対象とした。各 SVOC の μ-CTE からの回収率を図 2 に示した。

直径 64 mm の円形に裁断した検体を μ-CTE250i の不活性処理ステンレス製チャンバーに入れ、室温で 4 時間、高純度 He ガスを一定圧力 (流速約 50 ml/min) で通気した。この間、通気開始 10 分後から 3 時間 50 分にわたってガス状の放散化合物を不活性処理ステンレス製吸着管 (Tenax TA/ Carbograph 1TD/Carboxen 1000) で捕集した。

ついで、検体を除いて清浄なチャンバーに交換した後に、超高純度 He ガスを約 50 ml/min の流速で流しながらチャンバーを室温から 200℃まで 1 時間にわたって加熱し、チャンバー内の蓋部分に吸着した SVOC を脱離させて吸着管に捕集した。

B-4 加熱脱離-GC/MS による SVOC の定量

吸着管に捕集した SVOC は、加熱脱離-GC/MS (Shimadzu TDTS-2010 及び GCMS-2010) で定量した。主要な測定条件を以下に記した。

[TDTS-2010]
DESORPTION: 300°C, 10 min, 50 mL He/min
COLD TRAP: -10°C
TRAP DESORPTION: 300°C, 10 min
LINE and VALV TEMP.: 300°C
[GC]
COLUMN: Rtx-1 (0.32 mm x 60 m, 1μm)
CARRIER GAS: He, 30cm/min
SPLIT RATIO: 1:20
OVEN TEMP.: 80°C - (40°C/min) - 200°C – (5°C/min) - 320°C (5 min)
[MS]
INTERFACE TEMP.: 250°C
ION SOURSE TEMP.: 230°C
MONITOR IONs:
Triethyl Phosphate 155 (99, 127)
Tripropyl Phosphate 183 (99, 141)
TXIB 71 (43, 56, 83)
Tributyl Phosphate 211 (99, 155)
Tris(2-chloroethyl) Phosphate 249 (63, 251)
Dibutyl Adipate 129 (111, 185)
Dibutyl Phthalate 149 (150, 223)
Tris(1,3-dichloroisopropyl) Phosphate 209 (99, 211, 381)
Benzyl Butyl Phthalate 149 (91, 206)
Tri(butoxyethyl) Phosphate 299 (125, 199)
Bis(2-ethylhexyl) Adipate 129 (57, 147)
Triphenyl Phosphate 326 (77, 325)
Isodecyl Diphenyl Phosphate 251 (94, 250)
Di-n-octyl Phenyl Phosphate 175 (94, 287)
Tris(2-ethylhexyl) Phosphate 211 (99, 113)
Bis(2-ethylhexyl) Phthalate 149 (167, 279)
Di-n-octyl Phthalate 149 (150, 279)
Bis(2-ethylhexyl) Terephthalate 261 (112, 279)
Tris(2-chloroisopropyl) Phosphate 277 (125, 279)
Cresyl Diphenyl Phosphate 340 (77, 339)
Bis(4-methylphenyl) Phenyl Phosphate 354 (165, 353)
Dinonyl Adipate 255 (57, 129)
Tricresyl Phosphat 368 (107, 367)
DINCH 155 (127, 299)
Dinonyl Phthalate 293 (127, 149)
DBP-d4 153 (227)
BBP-d4 153 (210)
DEHP-d4 153 (283)
確認イオンを括弧内に示した。

C. 結果と考察

C-1 6 連チャンバー型 μ-CTE による VOC 放散試験 (平成 22 年度)

遮光、防音あるいは遮熱加工等の表記のある機能カーテン 12 製品、ジョイントマット 6 製品及びコルクマット 6 製品の計 24 製品について μ-CTE 法による放散試験を実施した。放散試験開始 2 時間後の TVOC 放散速度から容積 20 m^3、換気回数 0.5 回/h の室内に一定面積 (機能カーテンは 5 m^2、床用マットは 8 m^2 とした) の検体が存在した場合の TVOC 増加量を推算した結果、室内空気中の TVOC

濃度が 3,700～7,500 μg/m^3 まで顕著に増加する可能性があるという推算結果が得られた。

これらの製品から放散される VOCs を同定するために、放散試験開始 2 時間後の TVOC 測定結果についてデコンボリューション解析を行った結果、機能カーテンからは N,N-Dimethylformamide (3,000 μg/m^2/h)、Cyclohexanone (450 μg/m^2/h)、Toluene (430 μg/m^2/h)、ジョイントマットからは Formamide (2,100 μg/m^2/h) や Ethanoe 化合物、コルクマットから 2-Ethylhexyl Acrylate (3,300 μg/m^2/h) や 2-Ethyl-hexanol (570 μg/m^2/h)、2-Ethylhexyl Acetate (430 μg/m^2/h) の放散が暫定的に確認された。

C-2 4 連チャンバー型 μ-CTE 放散試験による VOC と SVOC の同時評価 (平成 23 年度)

カーペット製品からの TVOC 放散速度は 40～7,269 μg/m^2/h であった。容積 20 m^3、床面積 8 m^2、換気回数 0.5 回/h の室内の床一面にカーペットが敷き詰められている状態を想定して室内空気中濃度増分予測値を算出した結果、20 製品中の 13 製品で、製品の使用によって TVOC 暫定目標値 400 μg/m^2 を超える室内空気汚染を引き起こす可能性のあることが明らかになった (図 3)。

カーペットからの SVOC 放散速度を検討した結果、TCEP (35 μg/m^2/h)や DBA が 218 μg/m^2/h の放散速度で放出されることが明らかとなった。床面積 8 m^2 の室内を想定した場合、これらのカーペットが存在することによって 1 日当たりそれぞれ 6.7 mg、42 mg 程度の SVOC 負荷を生じるものと推定された。

C-3 4 連チャンバー型 μ-CTE 放散試験による形態別 SVOC 放散量の評価法 (平成 24 年度)

Wool 製 2 製品と Polyester 製 3 製品及び Rush 製 1 製品で TXIB の放散が認められ (1.9～24 μg/m^2/h)、大部分がガス態として放散された。Tributyl Phosphate は Acryl 製 2 製品と Polypropylene 製 1 製品で 40～47 μg/m^2/h の放散が認められ、20%前後が付着態として検出された。

Wool 製 1 製品、Acryl 製 1 製品、Nylon 製 2 製品から Bis(2-ethylhexyl) Phthalate の放散が認められ (1.1～4.2μg/m^2/h)、何れの製品からも全て付着態として放散された。Tris(2-chloroisopropyl) Phosphate は Acryl 製 1 製品と Nylon 製 1 製品、Polypropylene 製 1 製品から 10～11 μg/m^2/h の放散が認められ、大部分が付着態として検出された (図 4)。

試験を行ったカーペット製品を床面積 8 m^2、容積 20 m^3、換気回数 0.5 回/h の部屋の床に敷き詰めた場合を想定し、製品の使用に伴う室内空気中濃度の増加量 (気中濃度増分予測値) を推計した結果、Rush 製のカーペットを敷き詰めた場合は TXIB の空気中濃度は 16 μg/m^3 に達することが予想された。Tributyl Phosphate についても気中濃度増分予測値は 25～26 μg/m^3 となり、TXIB の場合と同様にカーペットが室内での継続的な放散源となる可能性が明らかになった。

一方、μCTE による放散試験において付着態で検出される SVOC は、実際の室内環境中ではカーペットの表面、あるいは表面に堆積したハウスダストに吸着して存在することが想定される。そこで、大部分が付着態として存在する Tris(2-chloroisopropyl) Phosphate について、Polypropyrene 製のカーペットで得られた 1 日あたりの室内環境への負荷量の最大値 268 μg/m^2 を用いて、Hand-to-Mouth 行動による経口暴露量の推計

を行った (幼児の体重: 10 kg、幼児の手の表面積: 10 cm^2、Hand –to-Mouse 行動の頻度: 5 回/h、1 日あたりの滞在時間: 8 時間、カーペット表面から手への移行率: 100%、手へ体内(口腔内) への移行率: 100%と仮定した)。その結果、幼児の Hand-to-Mouth 行動による Tris(2-chloroisopropyl) Phosphate 経口暴露量の推計値として 1.1 μg/kg/day が得られた。この値は Tris(2-chloroisopropyl) Phosphate の ADI 4 μg/kg/day の 1/4 を占めることになるが、今後は、移行率の初期値の設定も含めて Hand-to-Mouth 行動による適切な暴露シナリオの構築が必要であると考えられる。

D. 結論

本分担研究では、家庭用品から室内環境中へガス態及び付着態として放散される VOC 及び SVOC の定量的評価手法として μ-CTE 法を確立し、カーテンやカーペット等の家庭用品からの放散挙動を検討した。その結果、Cyclohexanone や Toluene 、2-Ethylhexyl Acrylate、2-Ethyl-hexanol、TXIB など、我々が実施した室内空気の全国調査において検出される様々な化学物質がこれらの家庭用品から放散されることが明らかになった。また、今後、ハウスダスト等を介した暴露が問題となる SVOC についても、Tris(2-chloroisopropyl) Phosphate や Bis(2-ethylhexyl) Phthalate の放散を定量的に評価できることが明らかになった。

本研究で確立した μ-CTE による SVOC の放散試験法では、ガス態として室内環境中に放散されてそのままの状態で、あるいは浮遊粒子状物質に吸着した状態で経気道暴露される可能性の高い Fraction と、製品表面や近傍へ移行した後に Hand-to-Mouth 行動やハウスダストの摂食による経口暴露、並びに直接的な接触による経皮暴露の可能性が高い fraction を分別して推計することが可能である。今後は、それぞれの経路による暴露シナリオを精緻化することによって、μ-CTE 放散試験の結果をもとに様々な家庭用品から放散される VOC/SVOC の多経路暴露スクリーニングが可能となることが期待される。

E. 健康危険情報

なし

F. 研究発表

1. 論文発表

なし

2. 学会発表

1) 古川 容子, 香川 (田中) 聡子, 田中 研次, 神野 透人, 西村 哲治: 機能カーテンから放散される揮発性有機化合物 - GC/TOFMS による網羅的解析 -. 平成22年度室内環境学会学術大会, 2010 年 12 月.
2) 岡元 陽子,香川(田中) 聡子,田中 研次,新井 悦恵,古川 容子,神野 透人,西村 哲治: 家庭用品から放散する準揮発性有機化合物のスクリーニング試験に関する研究 . 平成 23 年度室内環境学会学術大会, 2011 年 12 月.

G. 知的財産権の出願・登録状況

(予定を含む)

1. 特許取得

なし

2. 実用新案登録

なし

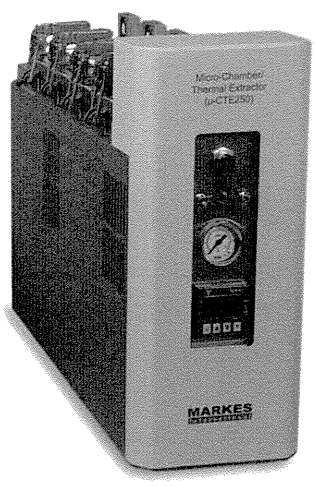

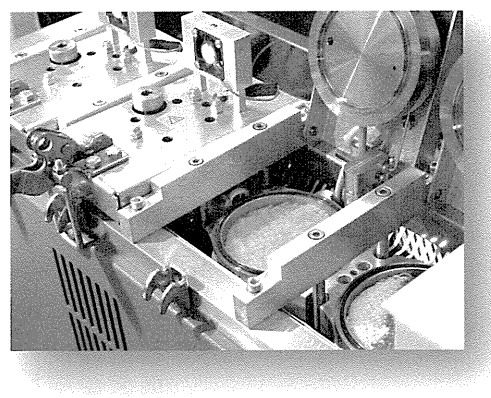

図 1　μ-CTE 250i 本体及び検体をセットしたチャンバーの外観

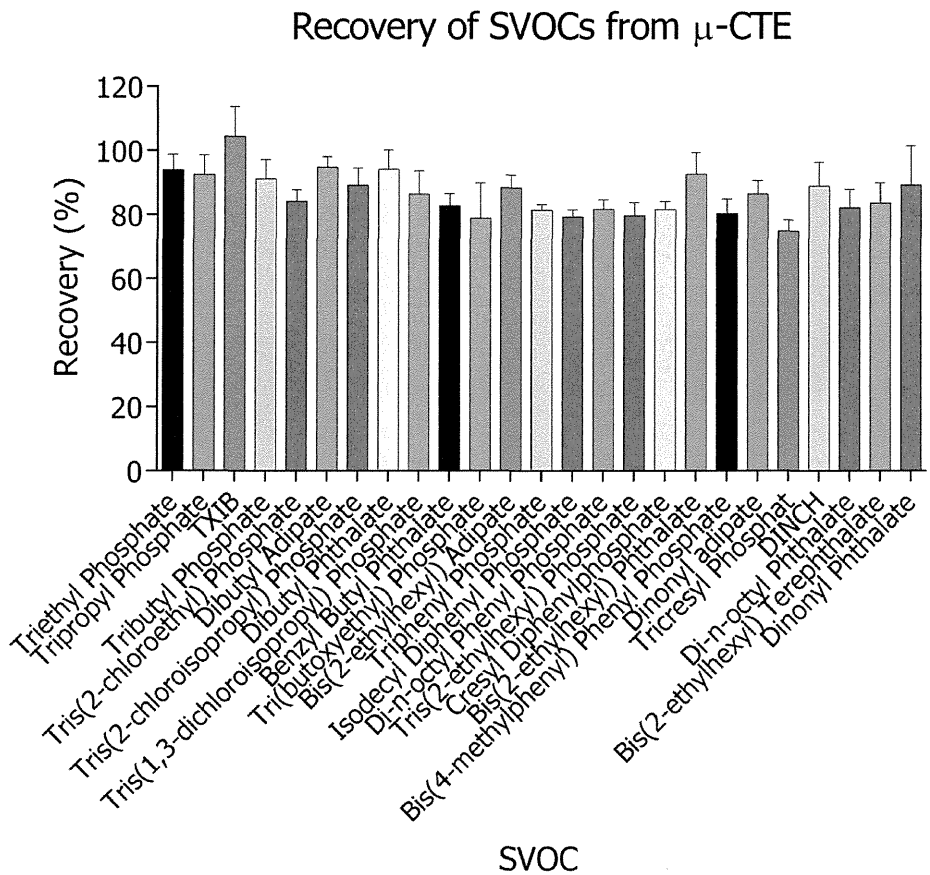

図 2　SVOC 25 化合物の μ-CTE からの回収率
(3 回の独立した実験の Mean ± SD を示した)

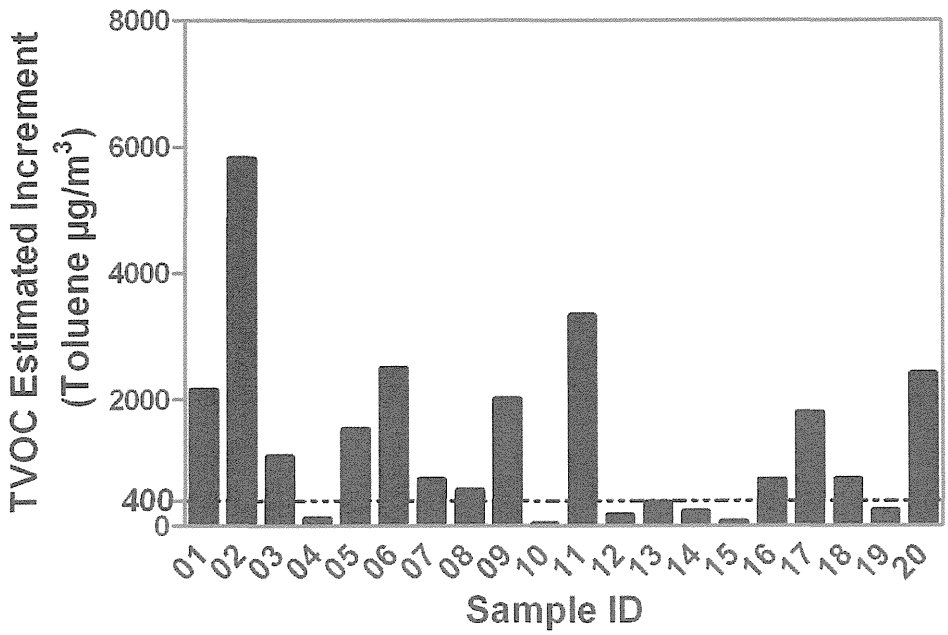

Number of values	20
Minimum	32.00
25% Percentile	228.3
Median	736.5
75% Percentile	2110
Maximum	5815
5% Percentile	33.50
95% Percentile	5691
Mean	1331
Std. Deviation	1436
Std. Error	321.1
Geometric mean	663.1

図3　カーペットから放散されるTVOCの室内空気中濃度増分予測値

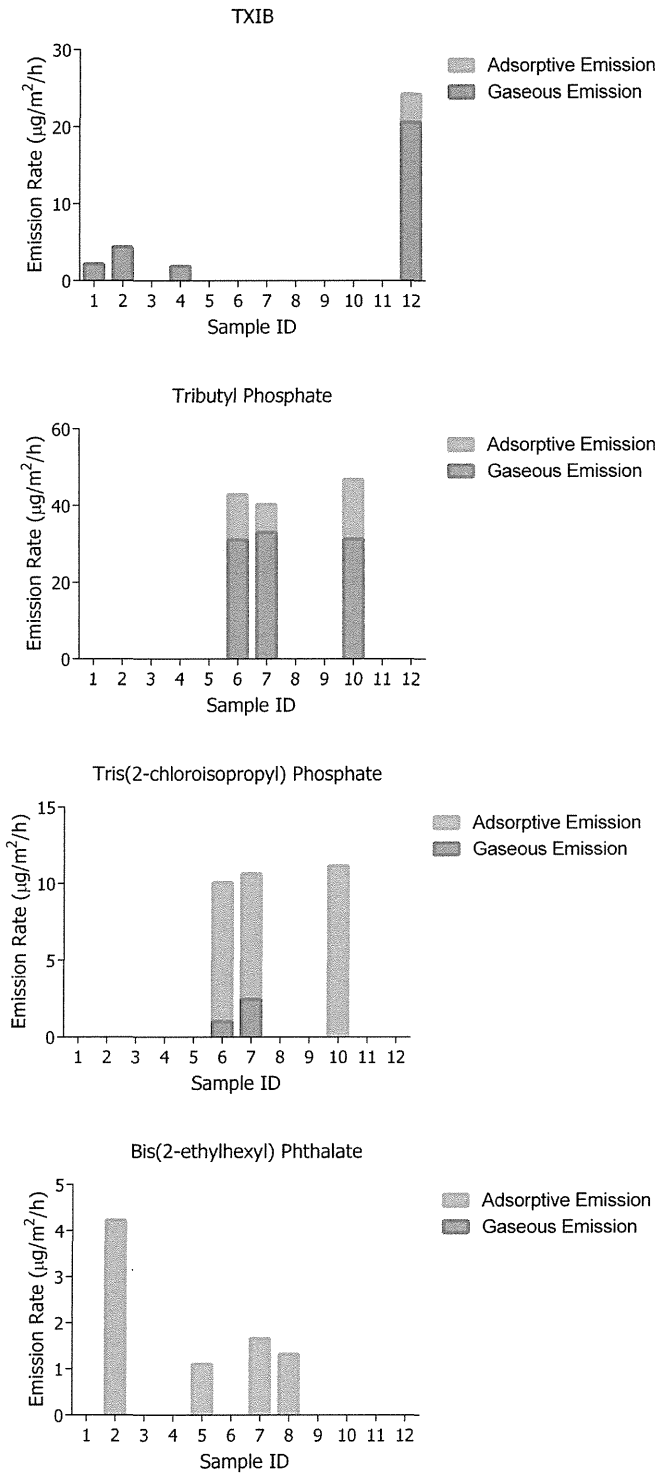

(TVOC 暫定目標値: 400 μg/m³)

図4　カーペットからの TXIB、Tributyl Phosphate、Tris(2-chloroisopropyl) Phosphate 及び Bis(2-ethylhexyl) Phthalate の放散速度

III. 研究成果の刊行に関する一覧表

研究成果の刊行に関する一覧表

発表者氏名	論文タイトル名	発表誌名	巻号	ページ	出版年
Ohkawara, S., Tanaka- Kagawa, T., Furukawa, Y., Nishimura, T. and Jinno, H.	Activation of the human transient receptor potential vanilloid subtype 1 by essential oils.	Biol. Pharm. Bull.	33	1434-1437	2010
Ohkawara, S., Tanaka- Kagawa, T., Furukawa, Y., Nishimura, T. and Jinno, H.	Development of a SYBR Green real-time polymerase chain reaction assay for quantitative detection of human N-methyl-D-aspartate receptors subtype 1 splice variants.	J. Health Sci.	56	527-533	2010
Miura, T. and Kumagai, Y.	Immunochemical method to detect proteins that undergo selective modification by 1,2-naphthoquinone derived from naphthalene through metabolic activation.	J. Toxicol. Sci.	35	843-852	2010
Miura, T., Shinkai, Y., Jiang, HY., Iwamoto, N., Sumi, D., Taguchi, K., Yamamoto, M., Jinno, H., Tanaka-Kagawa, T., Cho, AK. and Kumagai, Y.	Initial response and cellular protection through the Keap1/Nrf2 system during exposure of primary mouse hepatocytes to 1,2-naphthoquinone.	Chem. Res. Toxicol.	24	559-567	2011
Takayama, N., Iwamoto, N., Sumi, D., Shinkai, Y., Tanaka-Kagawa, T., Jinno, H. and Kumagai,Y.	Peroxiredoxin 6 is a molecular target for 1,2-naphthoquinone, an atmospheric electrophile, in human pulmonary epithelial A549 cells.	J. Toxicol. Sci.	36	817-821	2011
Ohkawara, S., Tanaka-Kagawa, T., Furukawa, Y. and Jinno, H.	Methylglyoxal activates the human transient receptor potential ankyrin 1 channel.	J. Toxicol. Sci.	37	831-835	2012
Hirose, R., Miura, T., Sha, R., Shinkai, Y., Tanaka-Kagawa, T. and Kumagai, Y.	A method for detecting covalent modification of sensor proteins associated with 1,4-naphthoquinone-induced activation of electrophilic signal transduction pathways.	J. Toxicol. Sci.	37	891-898	2012

IV. 研究成果の刊行物・別刷

Activation of the Human Transient Receptor Potential Vanilloid Subtype 1 by Essential Oils

Susumu OHKAWARA,[a] Toshiko TANAKA-KAGAWA,[b] Yoko FURUKAWA,[b] Tetsuji NISHIMURA,[b] and Hideto JINNO*,[b]

[a] *Department of Pharmaceutical Science, Musashino University; 1–1–20 Shinmachi, Nishitokyo, Tokyo 202–8585, Japan: and* [b] *Division of Environmental Chemistry, National Institute of Health Sciences; 1–18–1 Kamiyoga, Setagaya-ku, Tokyo 158–8501, Japan.* Received February 12, 2010; accepted May 26, 2010; published online June 4, 2010

Transient receptor potential vanilloid subtype 1 (TRPV1) is a non-selective cation channel activated by capsaicin. TRPV1 is expressed not only on human sensory neurons but also on human epidermal and hair follicle keratinocytes. Therefore, TRPV1 could have the potential to be a therapeutic target for skin disorders. To search for novel TRPV1 agonists, we screened 31 essential oils by using human TRPV1-expressing HEK293 cells. TRPV1 was activated by 4 essential oils: rose, thyme geraniol, palmarosa, and tolu balsam. The dose–response curves for TRPV1 activation by the essential oils revealed a rank order potency [the half-maximal effective concentration (EC_{50})] of rose>palmarosa>thyme geraniol>tolu balsam, and rank order efficiency (% activity in response to 1 μM capsaicin) of tolu balsam>rose>palmarosa>thyme geraniol. Moreover, the dose–response curves for TRPV1 activation by citronellol (main constituent of rose oil) and geraniol (main constituent of thyme geraniol and palmarosa oils) were consistent with the potency and efficiency of each essential oil. In contrast, benzyl cinnamate and benzyl benzoate (main constituent of tolu balsam oil) and geranyl acetate (main constituent of thyme geraniol oil) did not show TRPV1 activity. In this first-of-its-kind study, we successfully investigated the role of some essential oils in promoting human TRPV1 activation, and also identified two monoterpenes, citronellol and geraniol, as new human TRPV1 agonists.

Key words: transient receptor potential vanilloid subtype 1; monoterpene; essential oil

Transient receptor potential vanilloid subtype 1 (TRPV1) is a nonselective cation channel activated by capsaicin (a pungent ingredient of red pepper),[1] heat (>43 °C), acidic pH,[2] lipid,[3,4] and various natural products.[5—9] Although TRPV1 is known to be involved in peripheral nociception,[10,11] it is also widely expressed on human epidermal[12—14] and hair follicle keratinocytes.[15] In addition, TRPV1 signaling plays physiologically important roles in normal functioning of the human skin. Bodó *et al.* have recently provided the first evidence towards this with their discovery that TRPV1 activation promotes hair follicle regression, hair matrix keratinocyte apoptosis, inhibits hair matrix keratinocyte proliferation, and retards hair shaft elongation.[16] TRPV1 agonists have been recently proposed as therapeutic targets not only in acute neuropathic pain but also in skin disorders.[17]

Many plant-derived essential oils have been used traditionally to treat various skin disorders.[18] The medicinal use of essential oils that began in ancient Egypt has continued ever since and aromatherapy[19] has recently become popular worldwide. In addition, essential oils may provide a therapeutic alternative to western medicine.[20] However, the lack of a scientific basis evaluating the effectiveness of essential oils is an impediment to its increased use.

Essential oils are naturally occurring complex, multicomponent systems composed mainly of monoterpenes in addition to some non-terpene components.[21] Because TRPV1 is known to be activated by certain monoterpene, including camphor,[22] we speculated that the various pharmacological actions of essential oils may exercise through TRPV1.

The aim of this study was to search for novel compounds that activate human TRPV1, for which we screened 31 commercially available essential oils noted for their remedial properties against skin disorders.[18] This was achieved by measuring the intracellular Ca^{2+} concentration ($[Ca^{2+}]_i$) in human TRPV1-expressing HEK293 cells.

MATERIALS AND METHODS

Materials Capsaicin, capsazepine (CPZ), citronellol, geraniol, geranyl acetate, benzyl benzoate and dimethyl sulfoxide (DMSO) were purchased from Sigma-Aldrich Co. (St. Louis, MO, U.S.A.). Benzyl cinnamate was purchased from Tokyo Kasei Kogyo Co., Ltd. (Tokyo, Japan). Essential oils were purchased from PLANAROM International (Ghislenghien, Belgium).

Cloning of Human TRPV1 Oligo(dT) primed cDNA was synthesized from 5 mg of the total RNA isolated from human dorsal root ganglion (Clontech, Mountain View, CA , U.S.A.) using a SuperScript™ III first-strand synthesis system for reverse transcription-polymerase chain reaction (RT-PCR) (Invitrogen, Carlsbad, CA, U.S.A.) according to the manufacturer's instructions. An aliquot of the first cDNA (2 μl) was then subjected to PCR amplification with the use of Pfx DNA polymerase (Invitrogen) using the following primers 5′-CACCATGAAGAAATGGAGCAGC-3′ (N-terminal forward primer with CACC sequence) and 5′-CTTCTCCCCGGAAGCGGCAG-3′ (C-terminal reverse primer without the stop codon). The PCR products were then separated on a 0.7% agarose gel, and the bands were excised, purified using the MinElute Gel Extraction Kit (Qiagen, Valencia, CA, U.S.A.). Purified PCR products were subcloned into pENTR™/d-TOPO vector (Invitrogen) and named as hTRPV1-pENTR/d-TOPO. Next, hTRPV1-pENTR/d-TOPO was recombined with the pcDNA5/FRT mammalian expression vector (Invitrogen) using *attL* and *attR* reaction with Gateway™ LR Clonase™ enzyme mix (Invitrogen) and named as hTRPV1-pcDNA5/FRT.

Development of Human TRPV1-HEK293 Stable Cell

* To whom correspondence should be addressed. e-mail: jinno@nihs.go.jp

Line HEK293 cells containing FLP recombination site (Invitrogen) were cotransfected with hTRPV1-pcDNA5/FRT and pOG44 vectors (Invitrogen) using lipofectamine LTX (Invitrogen). Stable clones expressing TRPV1 were then selected using hygromycin B antibiotic selection and colonies were expanded to produce a large stock of TRPV1-expressing cells. TRPV1 protein expression was confirmed by Western blotting.

Western Blotting Cells were lysed in 200 μl of lysis buffer [20 mM Tris–HCl, 150 mM NaCl, 1 mM EDTA, 1% Triton X-100, and protease inhibitor cocktail (Sigma-Aldrich Co.), pH 7.5]. After 30 min of solubilization at 4 °C under agitation, lysates were centrifuged (16000 ***g***, 10 min, 4 °C). Protein extracts were diluted in 2× Laemmli buffer, resolved by SDS-polyacrylamide gel electrophoresis, and transferred to polyvinyliden difluoride membranes. Blocking was performed using 5% nonfat dry milk in Tris-buffered saline containing 0.1% Tween 20 followed by incubation with anti-V5-HRP antibody (diluted at 1 : 5000: Invitrogen) in the blocking buffer at 4 °C overnight. After a 15-min wash with Tris-buffered saline containing 0.1% Tween 20, membranes were incubated for 1 h with anti-rabbit horseradish peroxidase-conjugated secondary antibody (diluted at 1 : 1000) from GE Healthcare (Chalfont St. Giles, Buckinghamshire, U.K.). Chemifluorescence (enhanced chemiluminescence-plus; GE Healthcare, Piscataway, NJ, U.S.A.) was detected using the Typhoon 9400 Variable Mode Imager and ImageQuant analysis GE Healthcare.

Intracellular Calcium Measurement on the FlexStation Cells were plated at 80—90% confluence on 96-well, poly-D-lysine black-walled, clear-bottomed plates (Griner bio-one, Frickenhausen, Germany) 24 h prior to initiating the experiments. The cells were incubated for 1 h at 37°C in Hank's balanced salt solution (HBSS) buffer (HBSS plus 20 mM HEPES buffer, pH 7.4) containing FLIPR® calcium 4 assay reagent (Molecular Devices, Sunnyvale, CA, U.S.A.) followed immediately by fluorescence measurement. Fluorescence was measured using FlexStation (excitation at 485 nm and emission at 525 nm, using a 515 nm cut off) and SoftMax Pro 4.7.1 software (Molecular Devices). Experiments were performed at room temperature (30 °C). In some experiments, CPZ (10 μM) was added at least 1 min prior to the addition of the test compounds and essential oils. The test compound and essential oils were prepared in DMSO and add to the HBSS buffer (final DMSO conc. 0.2%). EC_{50} values were determined using Prism 4 software (GraphPad Software, La Jolla, CA, U.S.A.).

RESULTS AND DISCUSSION

Firstly, expression of human TRPV1 in cloned TRPV1-expressing HEK293 cells were confirmed by the Western blotting (Fig. 1A). TRPV1 positive bands were detected with apparent molecular weights of 95 kDa, and a highly glycosylated form of TRPV1 at 120 kDa, consistent with the previous report by Vos *et al.*[23] No bands were detected for TRPV1 from nontransfected HEK293 cells. In addition, capsaicin produced a dose-dependent increase in $[Ca^{2+}]_i$ levels in this cloned TRPV1-expressing HEK293 cells (Fig. 1B), an estimated EC_{50} of 0.0158 μM, similar to the values previously reported for human TRPV1 obtained using the FLIPR assay

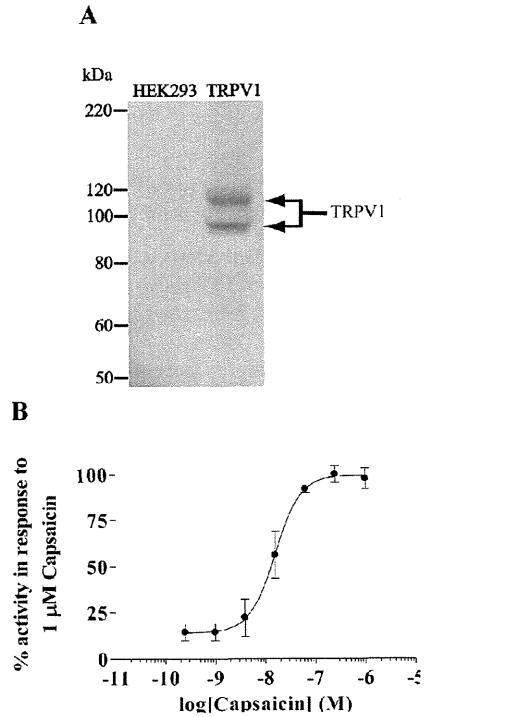

Fig. 1. TRPV1 Protein Stably-Expressed in HEK293 Cells Detected by Western Blotting

The band stands for TRPV1 protein fused with V5-epitope protein (A). The fusion protein was detected in chemiluminescence by anti-V5-HRP antibody. The molecular weight calculated from amino acid sequence is 95 and 125 kDa. Dose–response curves of capsaicin to elevate $[Ca^{2+}]_i$ in human TRPV1-expressing HEK293 cells (B). Data are expressed as percentage of the maximal effect observed with 1 μM capsaicin. Data are the mean±S.E. of at least three separate experiments.

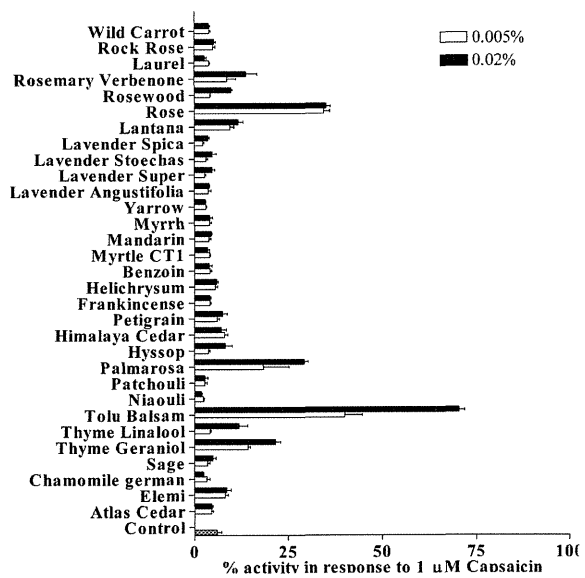

Fig. 2. The Effect of Essential Oils on $[Ca^{2+}]_i$ in Human TRPV1-Expressing HEK293 Cells

Data are expressed as the percentage of the maximal effect observed with 1 μM capsaicin. Data are mean±S.E. of at least three separate experiments.

(EC_{50} values of 0.0173 μM; Bianchi *et al.*[24]).

Next, thirty-one essential oils were examined at two concentrations (0.005, 0.02%) for TRPV1 activation by calcium imaging of TRPV1-expressing HEK293 cells (Fig. 2). We discovered four essential oils (thyme geraniol, tolu balsam, palmarosa, and rose) that increased $[Ca^{2+}]_i$ levels in TRPV1-

expressing HEK293 cells. The dose–response curves for TRPV1 activation by these essential oils revealed a rank order potency (EC_{50}) of rose (0.001%)>palmarosa (0.002%) >thyme geraniol (0.003%)>tolu balsam (0.005%) oils, and rank order efficiency (% activity in response to 1 μM capsaicin) of tolu balsam (61±4.5%)>rose (45±0.3%)>palmarosa (36±1.1%)>thyme geraniol (30±1.6%) oils (Fig. 3A). The response of these essential oils were inhibited by 10 μM CPZ (Fig. 3B) and were not observed in nontransfected HEK293 cells (data not shown), proving that these essential oils are specific agonists of human TRPV1.

To determine the specific essential oil constituents that contribute to the TRPV1 activation, we analyzed all oils and compared the activities of their main constituents. These constituents are listed in Table 1.

The dose–response curves for TRPV1 activation by citronellol (main constituent of rose oil), geraniol (main constituent of thyme geraniol and palmarosa oils) revealed a rank order potency of citronellol (43 μM)>geraniol (102 μM), and rank order efficiency of citronellol (45±4.9%)>geraniol (39±4.1%) (Fig. 4B). The response of these constituents were inhibited by 10 μM CPZ (Fig. 4C) and were not observed in nontransfected HEK293 cells (data not shown), proving that these essential oils are specific agonists of human TRPV1. Citronellol accounted for 39% with a concentration of 40 μM in 0.001% of rose oil as compared to geraniol which accounted for 39% and 78% with a concentration of 90 μM in 0.002% and in 0.003% of palmarosa and thyme geraniol oils, respectively. Consequently, because the potency and efficiency of citronellol and geraniol were consistent with that of essential oils, we concluded that human TRPV1 activation by rose, thyme geraniol, and palmarosa oils can be explained by the activity of each of their main constituents.

Geraniol has recently been described to activate rat TRPV1.[25] However, there are no reports evaluating the effect on geraniol on human TRPV1 activity accompanied by its EC_{50} value. Therefore, this study is the first of its kind to investigate these aspects. Apart from this, our findings also suggest that benzyl cinnamate and benzyl benzoate (main constituents of tolu balsam) do not affect TRPV1 activity. This is in conflict with the results for tolu balsam. Further investigation is required to elucidate the role played by each essential oil constituent in TRPV1 activation.

The activation of TRPV1 by capsaicin and other vanilloids is believed to occur *via* a non-covalent binding pocket in the transmembrane domain through π-stacking interactions between the aromatic moiety of Tyr 511 and the vanilloid ring moiety of capsaicin.[26] Allicin (garlic-derived sulfide components) also activate TRPV1[27] and recently they have been shown to activate by covalent binding to intracellular cysteine residue in the N-terminal region of TRPV1.[28] Although information regarding to citronellol and geraniol remain elu-

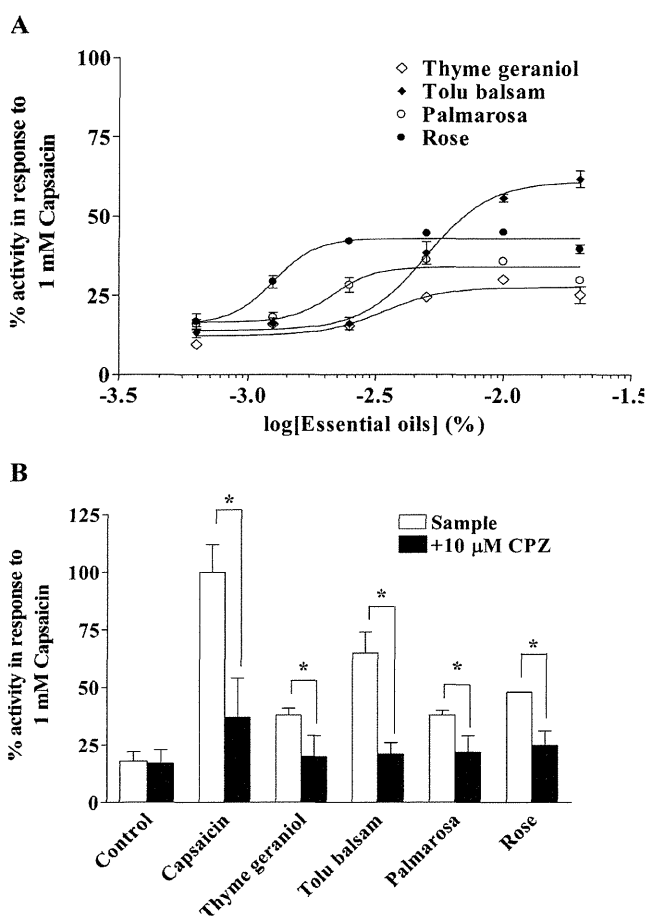

Fig. 3. Dose–Response Curves of Essential Oils to Elevate $[Ca^{2+}]_i$ in Human TRPV1-Expressing HEK293 Cells (A)

Data are expressed as percentage of the maximal effect observed with 1 μM capsaicin. Data are the mean±S.E. of at least three separate experiments. Effects of the TRPV1 CPZ on the responses of TRPV1-expressing HEK293 cells to essential oils (B). Data are the mean±S.E. of at least three separate experiments. $*p<0.01$ (unpaired t test).

Table 1. Main Constituent (%) of the 31 Essential Oils Analyzed in This Study

Essential oil	Main constituent (%)
Atlas cedar	β-Himachalen (49%)
Elemi	Limonene (51%)
Chamomile (German)	β-Farnesene (48%)
Sage	α-Thujone (29%)
Thyme geraniol	Geraniol (31%), Geranyl acetate (42%)
Thyme linalool	Linalool (80%)
Tolu balsam	Benzyl benzoate (57%), Benzyl cinnamate (29%)
Niaouli CT1	1,8-Cineol (50%)
Patchouli	Patchoulol (31%)
Palmarosa	Geraniol (78%)
Hyssop	β-Pinene (11%)
Himalaya cedar	β-Himachalen (37%)
Petigrain	Linalool (25%), Linalyl acetate (50%)
Frankincense	α-Pinene (32%)
Helichrysum	α-Pinene (27%)
Benzoin	Benzoic acid (15%)
Myrtle CT1	α-Pinene (59%)
Mandarin	Limonene (77%)
Myrrh	Curzerene (31%)
Yarrow	Camphor (14%)
Lavender angustifolia	Linalool (41%), Linalyl acetate (38%)
Lavender super	Linalool (37%), Linalyl acetate (31%)
Lavender stoechas	Fenchone (48%)
Lavender spica	Linalool (40%)
Lantana	β-Caryophyllene (13.4%)
Rose	Citronellol (39%)
Rosewood	Linalool (84%)
Rosemary verbenone	α-Pinene (28%)
Laurel	1,8-Cineol (47%)
Rock rose	Camphene (33%)
Wild carrot	α-Pinene (13%)

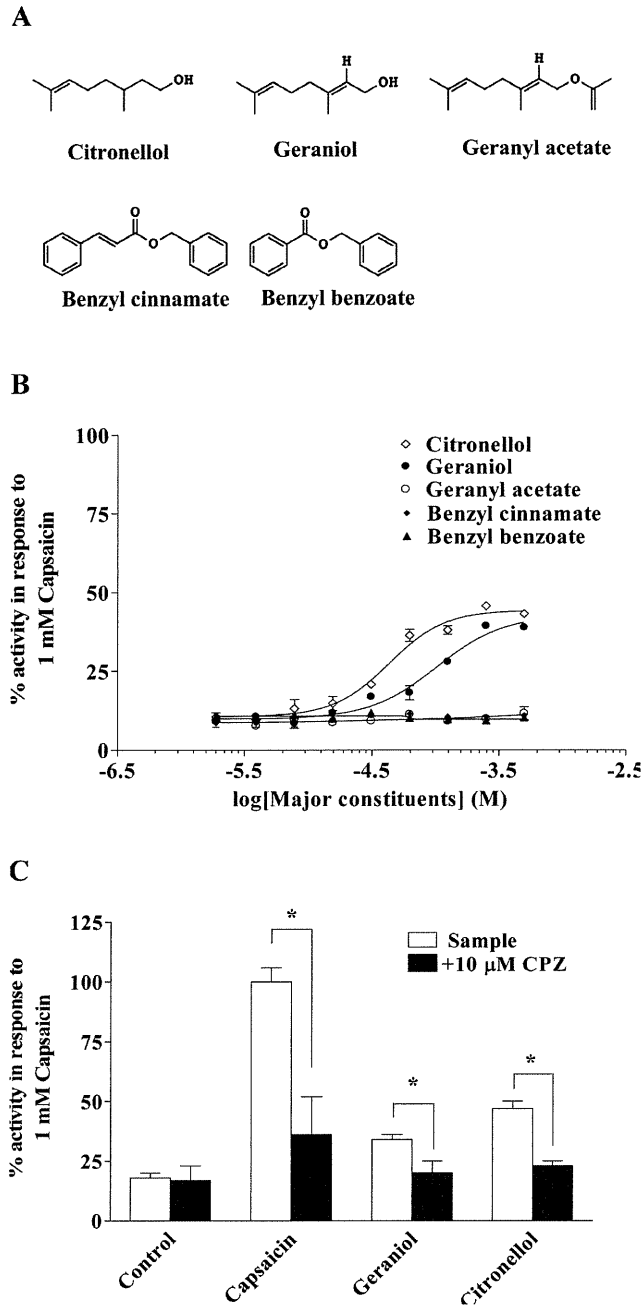

Fig. 4. Chemical Structure of the Major Essential Oils Constituents (Citronellol, Geraniol, Geranyl Acetate, Benzyl Benzoate, and Benzyl Cinnamate) (A) and $[Ca^{2+}]_i$ Dose–Response Curves of the Major Constituents of Essential Oils in Human TRPV1-Expressing HEK293 Cells (B)

Data are expressed as percentage of the maximal effect observed with 1 μM capsaicin. Data are the mean±S.E. of at least three separate experiments. Effects of the CPZ on the responses of TRPV1-expressing HEK293 cells to citronellol and geraniol (C). Data are the mean±S.E. of at least three separate experiments. $*p<0.01$ (unpaired t test).

sive, it has been shown that some monoterpenes could selectivity react to cysteine residue in bovine serum albumin.[29] Therefore, the mechanism of TRPV1 activation by citronellol and geraniol may similar that of *allicin*.

The human TRPV1 activity brought about by these oils has not been previously reported, and has been successfully investigated by this study. Apart from determining the effect exhibited by four essential oils, this study was also the first to reveal the effect of citronellol, the main constituent of rose oil, and geraniol, the main constituent of palmarosa and thyme geraniol oils, on human TRPV1 activity. Further detailed studies are required on the structure and physiological function of these active constituents to understand their potential as therapeutic remedies for various skin disorders.

Acknowledgement This work was supported in part by the Ministry of Education, Culture, Sports, Science, and Technology (MEXT), HAITEKU (2004—2008).

REFERENCES

1) Caterina M. J., Schumacher M. A., Tominaga M., Rosen T. A., Levine J. D., Julius D., *Nature* (London), **389**, 816—824 (1997).
2) Julius D., Basbaum A. I., *Proc. Natl. Acad. Sci. U.S.A.*, **97**, 8134—8139 (2001).
3) Huang S. M., Bisogno T., Trevisani M., Al-Hayani A., De Petrocellis L., Fezza F., Tognetto M., Petros T. J., Krey J. F., Chu C. J., Miller J. D., Davies S. N., Geppetti P., Walker J. M., Di Marzo V., *Proc. Natl. Acad. Sci. U.S.A.*, **99**, 8400—8405 (2002).
4) Van der Stelt M., Di Marzo V., *Eur. J. Biochem.*, **271**, 1827—1834 (2004).
5) Calixto J., Candida A. L., Kassuya E. A., Ferreira J., *Pharmaco. Ther.*, **106**, 179—208 (2005).
6) Sugai E., Morimitsu Y., Iwasaki Y., Morita A., Watanabe T., Kubota K., *Biosci. Biotechnol. Biochem.*, **69**, 1951—1957 (2005).
7) McNamara F. N., Randal A., Gunthorpe M., *Br. J. Pharmacol.*, **144**, 781—790 (2005).
8) Iwasaki Y., Morita A., Iwasawa T., Kobata K., Sekiwa Y., Morimitsu Y., Kubota K., Sekiwa Y., Watanabe T., *Nutr. Neurosci.*, **9**, 169—178 (2006).
9) Riera C. E., Menozzi-Smarrito C., Affolter M., Michlig S., Munari C., Robert F., Vogel H., Simon S. A., Coutre le J., *Br. J. Pharmacol.*, **157**, 1398—1409 (2009).
10) Tominaga M., Caterina M. J., Malmberg A. B., Rosen T. A., Gilbert H., Skinner K., *Neuron*, **21**, 531—543 (1998).
11) Di Marzo V., Blumberg P. M., Szallasi A., *Curr. Opin. Neurobiol.*, **12**, 372—379 (2002).
12) Denda M., Fuziwara S., Inoue K., Denda S., Akamatsu H., Tomitaka A., *Biochem. Biophys. Res. Commun.*, **285**, 1250—1252 (2001).
13) Inoue K., Koizumi S., Fuziwara S., Denda S., Inoue K., Denda M., *Biochem. Biophys. Res. Commun.*, **291**, 124—129 (2002).
14) Ständer S., Moormann C., Schumacher M., Buddenkotte J., Artuc M., Shpacovitch V., *Exp. Dermatol.*, **13**, 129—139 (2004).
15) Bodó E., Kovács I., Telek A., Varga A., Paus R., Kovács L., *J. Invest. Dermatol.*, **123**, 410—413 (2004).
16) Bodó E., Bíró T., Telek A., Czifra G., Telek A., Tóth B. I., *Am. J. Pathol.*, **166**, 985—998 (2005).
17) Harada N., Okajima K., *Growth Horm. IGF Res.*, **17**, 171—176 (2007).
18) Kerr J., *Int. J. Aromather.*, **12**, 202—206 (2003).
19) Rose J., Hulburd, J., *North Atlantic Books*, **1992**, 25—27 (1992).
20) Lis-Balchin M., *Pharmaceut. Press*, **2006**, 281—285 (2006).
21) Edris A. E., *Phytother. Res.*, **21**, 308—323 (2007).
22) Xu H., Blair N. T., Clapham D. E., *J. Neurosci.*, **28**, 8924—8937 (2005).
23) Vos M. H., Neelands T. R., McDonald H. A., Choi W., Kroeger P. E., Puttfarcken P. S., Faltynek C. R., Moreland R. B., Han P., *J. Neurochem.*, **99**, 1088—1102 (2006).
24) Bianchi B. R., Lee C. H., Jarvis M. F., El Kouhen R., Moreland R. B., Faltynek C. R., Puttfarcken P. S., *Eur. J. Pharmacol.*, **537**, 20—30 (2006).
25) Stotz S. S., Vriens J., Martyn D., Clardy J., Clapham1 D. E., *PloSONE*, **7**, e2082 (2008).
26) Jordt S. E., Julius D., *Cell*, **108**, 421—430 (2002).
27) Macpherson L. J., Geierstanger B. H., Viswanath V., Bandell M., Eid S. R., Hwang S., Patapoutian A., *Curr. Biol.*, **15**, 929—934 (2005).
28) Salazar H., Llorente I., Jara-Oseguera A., Garcia-Villegas R., Munari M., Gordon S. E., Islas L. D., Rosenbaum T., *Nat. Neurosci.*, **11**, 255—261 (2008).
29) Sasai T., Hirano Y., Maeda S., Matsunaga I., Otsuka A., Morita D., Nishida R., Nakayama H., Kuwahara Y., Sugita M., Mori N., *Biochem. Biophys. Res. Commun.*, **375**, 336—340 (2008).

— Regular Article —

Development of a SYBR Green Real-time Polymerase Chain Reaction Assay for Quantitative Detection of Human *N*-methyl-D-aspartate Receptors Subtype 1 Splice Variants

Susumu Ohkawara,[a] Toshiko Tanaka-Kagawa,[b] Yoko Furukawa,[b] Tetsuji Nishimura,[b] and Hideto Jinno*,[b]

[a]*Department of Pharmaceutical Science, Musashino University, 1–1–20 Shinmachi, Nishitokyo-shi, Tokyo 202–8585, Japan and* [b]*Division of Environmental Chemistry, National Institute of Health Sciences, 1–18–1 Kamiyoga, Setagaya-ku, Tokyo 158–8501, Japan*

(Received February 23, 2010; Accepted July 7, 2010; Published online July 23, 2010)

N-methyl-D-aspartate receptors (NMDAR) belong to the ionotropic glutamate receptor subclass and are widely distributed in the vertebrate brain. Molecular cloning has revealed the existence of seven NMDAR subunits: one NMDAR1 (NR1), four different NMDAR2 (NR2A-D), and two different NMDAR3 (NR3A,B). Alternative splicing of the single NR1 gene generates eight isoforms with distinct functional properties. So far, the transcripts of the NR1 splice variants have been discriminated by Northern blot, *in situ* hybridization, or competitive polymerase chain reaction (PCR) methods all of which have their intrinsic limitations. In this study, we have developed a method to quantify the mRNAs of the NR1 splice variants by real-time PCR with the double-stranded DNA-binding dye SYBR Green I. The implementation of this assay will allow a better understanding of the regulatory mechanisms of the NR1 splice variants, and hence, their role in neuronal disease pathogenesis.

Key words —— *N*-methyl-D-aspartate, splice variants, real-time polymerase chain reaction

INTRODUCTION

Glutamate receptors are the primary mediators of excitatory synaptic transmission in the mammalian brain.[1] The *N*-methyl-D-aspartate (NMDA) subtype of glutamate receptor has been implicated in several critical central nervous system functions, including learning and memory.[2] NMDA receptor (NR) abnormalities may underlie a number of pathological conditions.[3] The molecular cloning studies showed that NR consists of three subunits named NR1,[4] NR2A-D,[5,6] and NR3A,B.[7–9] Furthermore, functional studies have revealed that NR1 subunits need to be coexpressed with NR2 subunits in order to produce cation transport activity.[10]

The human NR1 (hNR1) subunit mRNA is alternatively spliced at three exons to form eight splice variants.[11,12] Splicing of the *N*-terminal cassette (exon 4) results in NR1-a (absence) or NR1-b (presence) variants. In the *C*-terminal tail, individual splicing of the C1 (exon 20) or C2 (exon 21) cassette results in transcripts designated as NR1-2 or NR1-4, respectively. The presence or absence of both C1 and C2 cassettes results in NR1-1 and NR1-3 splice variants, respectively. Furthermore, the deletion of the C2 cassette alters the reading frame, generating an unrelated sequence of 22 amino acids designated as C2 .[13] These alternatively spliced regions of NR1 regulates the sensitivity to physiological pH,[14] and influences protein interactions[15] and intracellular trafficking.[16] Various studies have also shown that these splice variants vary in Alzheimer disease,[17,18] schizophrenia,[19] aging,[20] and exposure to various chemicals.[21–23] Hence, examination of the expression of the NR1 splice variants is crucial for determining their potential relevance in neurological diseases.

Evaluation of NR1 splice variants expression in these conditions presents critical restrictions and has been limited to research protocols partly due to analytical difficulties. Methods employed so far include Northern blotting,[21] *in situ* hybridization,[23]

*To whom correspondence should be addressed: Division of Environmental Chemistry, National Institute of Health Sciences, 1–18–1 Kamiyoga, Setagaya-ku, Tokyo 158–8501, Japan. Tel.: +81-3-3700-9298; Fax: +81-3-3700-9298; E-mail: jinno@nihs.go.jp

Table 1. Sequence of Oligonucleotides Used as Primers

mRNA target	Primer name	Sequence	Amplicon size
NR1-1	NR1-1/2F	5 -CTGGGATCTTCCTCATTTTCATC-3	128 bp
	NR1-1R	5 -CAGTGGGATGGTACTGCTGC-3	
NR1-2	NR1-1/2F	5 -CGGGATCTTCCTGATTTTCATC-3	123 bp
	NR1-2R	5 -CCCCCGGTGCTCTGCA-3	
NR1-3	NR1-3/4F	5 -GATAGAAAGAGTGGTAGAGCAGAGC-3	122 bp
	NR1-3R	5 -ACCCCCGGTGCTCGTG-3	
NR1-4	NR1-3/4F	5 -GATAGAAAGAGTGGTAGAGCAGAGC-3	126 bp
	NR1-4R	5 -CAGTGGGATGGTACTGCGTG-3	
NR1-a	NR1-aF	5 -GGAGCGTGAGTCCAAGGC-3	117 bp
	NR1-aR	5 -GGCAGAAAGGATGATGACCC-3	
NR1-b	NR1-bF	5 -AACTATGAAAACCTCGACCAACTG-3	83 bp
	NR1-bR	5 -GGTCCCTGGGTCAAACTGC-3	

and competitive PCR.[24] These methods provide only qualitative or semi-quantitative information, and a truly quantitative and reproducible evaluation of NR1 splice variants expression is still needed.

This study aimed to develop a reliable and accurate real-time PCR method using SYBR Green I dye that allows cost effective measurement of NR1 splice variants expression levels.

MATERIAL AND METHODS

cDNA Synthesis —— The human hippocampus PolyA$^+$ RNA (500 ng) from Clontech (Mountain View, CA, U.S.A.) was reverse transcribed using SuperScript III Reverse transcriptase and random hexamers (Invitrogen, Carlsbad, CA, U.S.A.). In addition, total RNA (5 μg) from a normal hippocampus and Alzheimer disease hippocampus obtained from BioChain (Hayward, CA, U.S.A.) were reverse transcribed using High-Capacity cDNA Archive Kit (Applied BioSystems, Foster City, CA, U.S.A.).

Primer Design —— Primers were purchased from Invitrogen and were designed using the Primer Premier software (PREMIER Biosoft International, Palo Alto, CA, U.S.A.). Two forward primers designated hNR1-1/2F and hNR1-3/4F, and four reverse primers designated hNR1-1R (four bases annealing to the 3 end of exon 19), hNR1-2R (five bases annealing to the 3 end of exon 19), hNR1-3R, and hNR1-4R (four bases annealing to the 3 end of exon 20), were designed to permit discrimination between the C-terminal splice variants. Two forward primers designated hNR1-aF and hNR1-bF, and two reverse primers designated hNR1-aR and hNR1-bR (two bases annealing to the 5 end of exon 5) were designed to permit discrimination between the *N*-terminal splice variants. The real-time PCR primer sequences are shown in Table 1.

Plasmid Standard —— A 164-bp NR1-1 sequence (GenBank accession no. NM 000832.5, 2478–2658 bp); 230-bp NR1-2 sequence (GenBank accession no. NM 021569.2, 2478–2706 bp); 341-bp NR1-3 (GenBank accession no. NM 007327.2, 2478–2817 bp); 274-bp NR1-4 (GenBank accession no. U08106.1, 2478–2769 bp); 257-bp NR1-a (GenBank accession no. NW017008, 439–694 bp); and 320-bp NR1-b (GenBank accession no. NW017008, 439–757 bp) were amplified from the hippocampus cDNA by PCR. The PCR products were then separated on 1% agarose gel, and the bands were excised, purified using the MinElute Gel Extraction Kit (Qiagen, Valencia, CA, U.S.A.), and cloned in the pCR4-TOPO vector of TOPO TA Cloning Kit (Invitrogen) as per the standard protocols. Plasmid cDNA constructs were prepared with the QIAprep Spin Miniprep Kit (Qiagen) and their identity was verified by DNA sequencing on a 3700 sequencer (Applied BioSystems). Plasmid cDNA concentrations were measured by UVmini-1240 absorbance spectrophotometer (Shimadzu, Kyoto, Japan). Serial dilutions of the extract were prepared containing 10^7–10^3 copies of the plasmid.

Real-time Quantitative PCR Using SYBR Green I —— Real-time PCR was performed on a SDS7000 (Applied BioSystems). The dilution series of the standard plasmid DNA for each hNR1 splice variant and 100 ng cDNA (total RNA equivalent) of samples was amplified in a 50 μl reaction containing 1 × SYBR Green I Master Mix (Applied BioSystems) and 50 nM of each primer and nuclease-free water. We performed

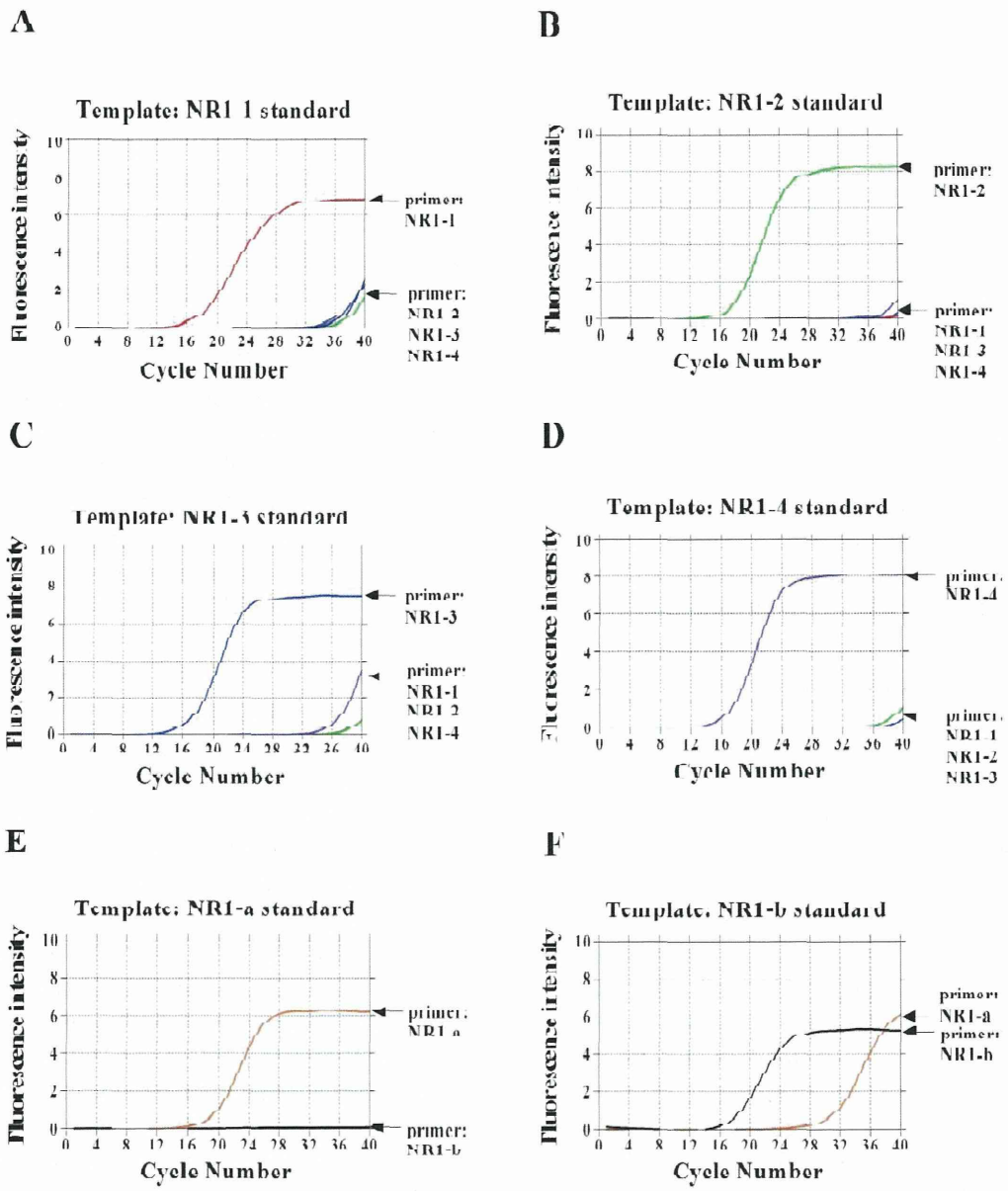

Fig. 1. Amplification Plots of SYBR Green I, Real-time PCR for Human NR1 Splice Variants

PCR was carried out using primers specific for NR1-1 (A), NR1-2 (B), NR1-3 (C), NR1-4 (D), NR1-a (E) and NR1-b (F) in the presence of each standard plasmids containing each splice variant specific cDNA sequence.

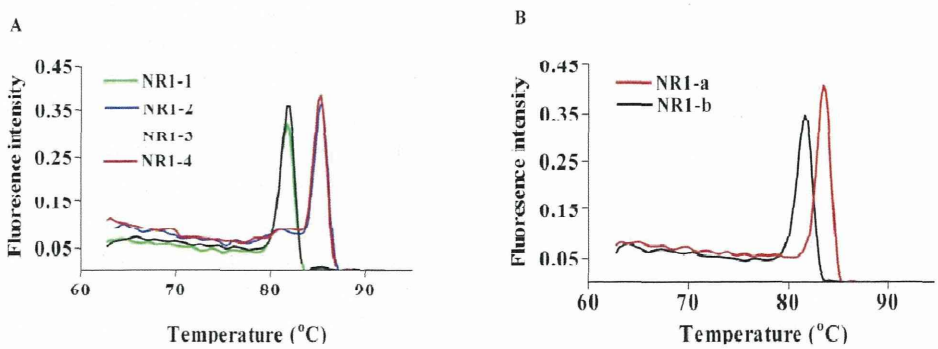

Fig. 2. Dissociation Curve Analysis of hNR1 Splice Variant Amplicons

A C-terminal splice variant amplicon (A) and *N*-terminal splice variant (B) is subjected to melting curve analysis and a plot of fluorescence versus temperature is indicated. The presence of a single peak is consistent with the formation of a single amplicon. It also indicates the lack of primer-dimer formation.

each amplification three times. The thermal profile consisted of one cycle at 95°C for 10 min followed by 40 cycles at 95°C for 15 s and at 62°C for 1 min. Melting curves were generated after amplification. Real-time PCR efficiencies for each reaction were calculated using the formula: efficiency (E) = $[10^{(1/\text{slope})}] - 1$, from the slope values given in the SDS7000.

Quantification and Data Analysis —— For each run, data acquisition and analysis was done by the SDS7000 System software. The relative mRNA level of each hNR1 splice variants was determined by interpolating the threshold cycle (Ct) values of the unknown samples to each standard curve and the obtained values were normalized to glyceraldehyde-3-phosphate-dehydrogenase (GAPDH) mRNA levels in same samples as determined by a TaqMan human GAPDH Control Reagent kit (Applied BioSystems).

RESULTS AND DISCUSSION

Specific detection of different hNR1 splice variants was achieved with the following primer pairs: NR1-1, primer pair NR1-1/2F-NR1-1R; NR1-2, primer pair NR1-1/2F-NR1-2R; NR1-3, primer pair NR1-3/4F-NR1-3R; NR1-4, primer pair NR1-3/4F-NR1-4R; NR1-a, primer pair NR1-aF-NR1-aR; and NR1-b, primer pair NR1-bF-NR1-bR. For every splice variant, 10^7 copies of standard plasmid cDNA were detectable with the appropriate primer sets with a mean Ct of 16. Real-time reverse transcription (RT)-PCR with "nonspecific" primer set for NR1-1, NR1-2, NR1-3, NR1-4, and NR1-a, and 10^7 copies of standard plasmid cDNA did not generate any reporter fluorescence signal even after 35 PCR cycles. On the other hand, real-time RT-PCR for NR1-b standard plasmid cDNA generated a reporter fluorescence signal in 28 cycles, and achieved a 8000-fold specificity with standard plasmid cDNA (Fig. 1). Specificity was also confirmed in a melting curve analysis performed on the SDS7000 (Fig. 2). Dissociation curves showed a single peak corresponding to a melting temperature of 81.6°C for NR1-1 and NR1-3, and corresponding to 85.3°C for NR1-2 and NR1-4 splice variants (Fig. 2A). Similarly, dissociation curves showed a single peak corresponding to melting temperatures of 83.5 and 81.6°C for NR1-a and NRI-b, respectively (Fig. 2B). These results demonstrate specific amplification and the absence of primer dimers.

To quantify the number of molecules of each hNR1 splice form, we constructed six different standard curves (Fig. 3). A linear relationship was observed between the initial copy numbers and each 10-fold dilution from 10^7–10^3 copies per reaction mixture, and the Ct values for each standard curve. A regression analysis of the Ct values generated by the log10 dilution series resulting in a correlation coefficient (r^2) value > 0.99 was performed for each standard curve. The efficiency of the PCR reaction was typically > 87%.

We also examined the relative expression (%) of hNR1 splice variants, *i.e.*, the ratio of a specific variant to the sum of all hNR1 splice variant mRNAs in hippocampus from normal and Alzheimer disease patients. In normal hippocampus, the relative expression of C-terminal splice variants was 47, 6, 30, and 17% for NR1-1, NR1-2, NR1-3, and NR1-4, respectively; in hippocampus of Alzheimer patients, the relative expression was 32, 9, 37, and 21% for NR1-1, NR1-2, NR1-3, and NR1-4, respectively (Table 2), suggesting similar expression patterns between the two groups. This result was in accordance with those of previous studies that used a different technology namely competitive PCR.[24] On the other hand, we found different expression patterns of the N-terminal splice variants between the hippocampus from normal and Alzheimer patients (Table 3). We observed that, in normal patients the percentage of NR1-a and NR1-b, as part of total N-terminal splice variants, was 84 and 16%, while in the Alzheimer patient the percentage was 39 and 61%, respectively. However, it must be noted that these mRNA samples were from single donors and hence the issue of interindividual variation has not been addressed in this study.

As NR involvement has been implicated in a number of pathologic conditions and as these conditions may be reflected in altered patterns of NR1 mRNA expression, quantification of mRNA expression is essential for the assessment of NR1-mediated mechanisms. A number of different methods are used for the quantification of mRNA, such as competitive RT-PCR, Northern blotting, and *in situ* hybridization. Of all these methods, competitive RT-PCR has proven to be the most accurate and sensitive method to study NR1 splice variant mRNA expression in the brains of Alzheimer patients.[24] However, this method has some drawbacks such as post-PCR manipulations, impaired quantification due to either a lack of sensitivity in gel quantification, variations in PCR efficiencies between in-

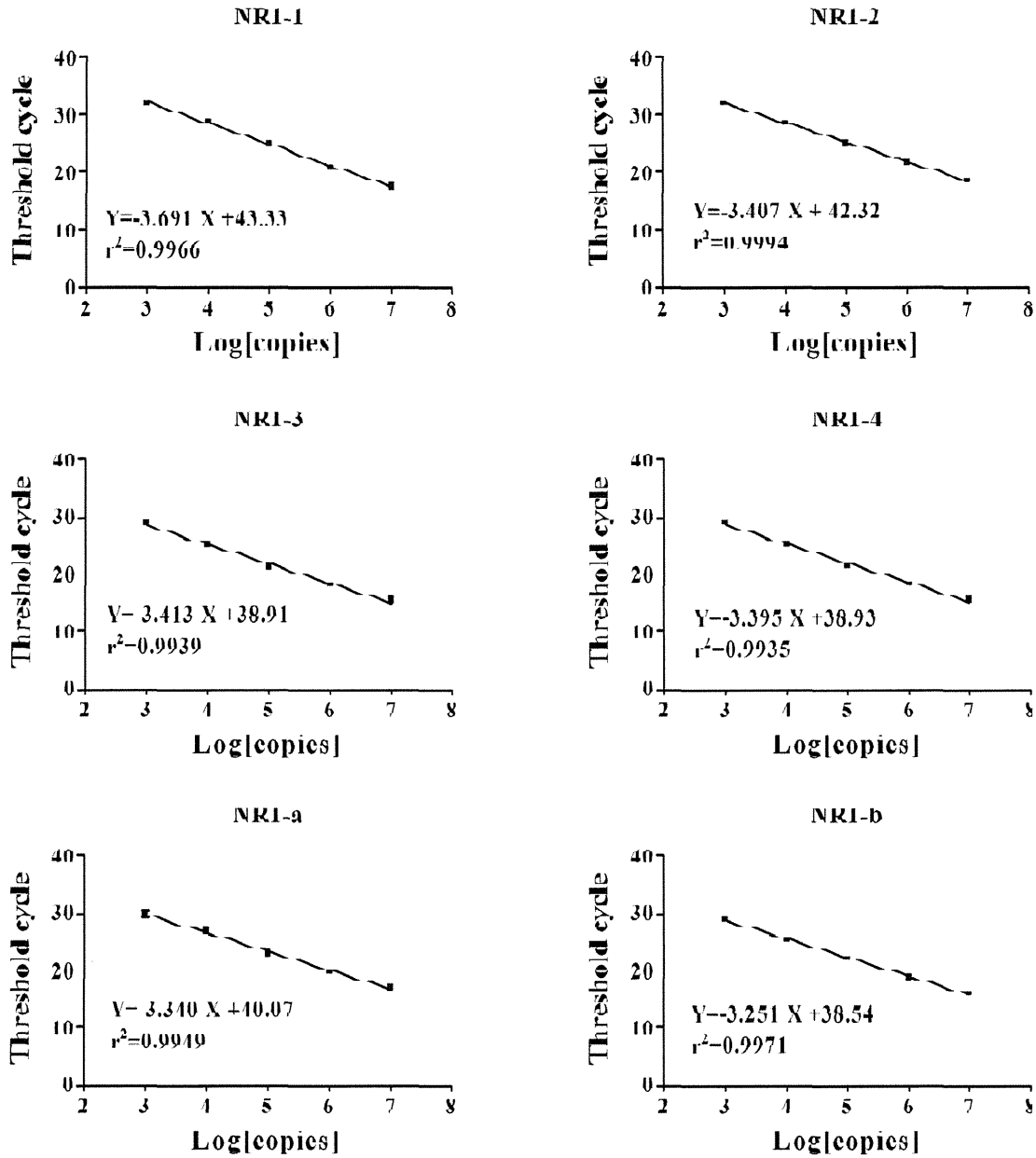

Fig. 3. Standard Curve for the Real-time PCR Amplification of Human NR1 Splice Variants

A plot of *Ct* values versus the logarithm of 10^3, 10^4, 10^5, 10^6, and 10^7 copies of standard plasmids containing the specific cDNA sequence for each splice variant is indicated.

Table 2. Expression of *C*-terminal NR1 Splice Variants mRNA in Normal and Alzheimer Patients Hippocampus

	Normal	Alzheimer
NR1-1	0.47 (47%)	0.32 (32%)
NR1-2	0.07 (6%)	0.09 (9%)
NR1-3	0.30 (30%)	0.37 (37%)
NR1-4	0.17 (17%)	0.22 (22%)

All data presented as the *C*-terminal NR1 splice variant: GAPDH mRNA ratio. The relative amounts of the individual splice variants related to the total sum are given in parentheses as percentages.

Table 3. Expression of *N*-terminal NR1 Splice Variants mRNA in Normal and Alzheimer Patients Hippocampus

	Normal	Alzheimer
NR1-a	0.63 (84%)	0.31 (39%)
NR1-b	0.12 (16%)	0.49 (61%)

All data presented as the *N*-terminal NR1 splice variant: GAPDH mRNA ratio. The relative amounts of the individual splice variants related to the total sum are given in parentheses as percentages.